

Investigations of dislocation patterns within grains and near grain boundaries in copper by the electron channelling contrast technique in scanning electron microscopy

By Z. F. ZHANG and Z. G. WANG

State Key Laboratory for Fatigue and Fracture of Materials, Institute of Metal Research, Academia Sinica, Shenyang, 110015, PR China

[Received in final form 7 April 1998 and accepted 8 April 1998]

ABSTRACT

In order to reveal the effect of grain boundaries (GBs) on cyclic deformation, the cyclically saturated dislocation patterns within grains and in the vicinity of GBs in a copper bicrystal with a large-angle GB and a copper multicrystal containing small-angle GBs have been observed by the electron channelling contrast technique in scanning electron microscopy. The observations for the multicrystal show that dislocation walls and persistent slip bands (PSBs) can transfer through the small-angle GBs. However, in the copper bicrystal with a large-angle GB perpendicular to the stress axis, PSBs can only form within the component grain with a relatively higher Schmid factor and cannot pass through the GB. From the experimental observations, the effect of GBs on cyclic deformation behaviour is discussed.

§ 1. INTRODUCTION

Single-crystal copper oriented for single slip exhibits three different regions in its cyclic stress–strain curve (CSSC) over a wide range of plastic strains and the saturation resolved shear stress of the plateau region (region B) maintains a constant value in the range 28–30 MPa (Mughrabi 1978, Cheng and Laird 1981). Correlation between the saturation dislocation patterns and the three regions in the CSSC has been well established (Mughrabi 1978, Laird *et al.* 1986). Dislocation structures induced by cyclic deformation are generally observed by transmission electron microscopy (TEM). TEM investigations require thin foil specimens and therefore the bulk specimen has to be destroyed. It is impossible to study the evolution of dislocation structure during the deformation of a single bulk specimen by TEM. In addition, TEM requires tedious specimen preparation and permits only a relatively small specimen area to be investigated.

Recently, the electron channelling contrast (ECC) technique in scanning electron microscopy (SEM) has been applied to study the dislocation patterns in cyclically deformed metals such as nickel (Schwab *et al.* 1996, 1998, Bretschneider *et al.* 1997), copper (Melisova *et al.* 1997, Li *et al.* 1998) and stainless steel (Zauter *et al.* 1992). In comparison with TEM, the SEM ECC technique has shown many attractive features. This technique has been found to be extremely suitable for studying the dislocation arrangements over a large specimen area and at some special sites, for example in the vicinity of grain boundaries (GBs), within deformation bands (Li *et al.* 1998) and ahead of cracks. It is well established that the saturation plateau observed in the CSSC is associated with the localization of the plastic deformation in

persistent slip bands (PSBs). Thus, PSBs are considered to be one kind of fatigue damage over a wide range of plastic strain amplitude. Meanwhile, GBs are favourable sites for fatigue crack initiation in polycrystalline materials under cyclic loading. It is necessary to reveal the plastic strain localization in PSBs and the interaction of PSBs with GBs for a better understanding of fatigue damage mechanisms in polycrystalline materials. Although the dislocation arrangements in PSBs have been studied by the SEM ECC technique, the interaction of PSBs with GBs has not been investigated by this technique.

§ 2. EXPERIMENTAL DETAILS

In the present study, a copper bicrystal with a large-angle GB and a multicrystal containing some small-angle GBs were grown from OFHC copper of 99.999% purity by the Bridgman method in a horizontal furnace. Fatigue specimens were spark machined from the as-grown crystals. Their orientations were determined by the Laue back-reflection technique. The stress axis orientation of the multicrystal specimens was $[123]$ on average. GBs in the multicrystal specimens were closely parallel to the stress axis and the misorientation between adjacent grains was about $3-5^\circ$. The stress axis orientations of the two component crystals in the bicrystal specimen were determined to be G1 $[5913]$ and G2 $[579]$ respectively. The GB plane in the bicrystal specimen was perpendicular to the stress axis. Before cyclic deformation, all the specimens were carefully electropolished for surface observation. Symmetrical push-pull tests were performed on a Shimadzu servohydraulic testing machine under constant-plastic-strain control at room temperature in air. A triangular wave with a frequency in the range 0.03–0.3 Hz was used. After cyclic saturation, the surface slip traces of the specimen were removed by electropolishing and then the dislocation patterns within grains and in the vicinity of GBs were observed by the SEM ECC technique. The operating conditions are listed in table 1.

§ 3. RESULTS

3.1. Saturation dislocation patterns in a copper multicrystal

Figure 1 shows the CSSCs of the copper multicrystal and of a copper single crystal oriented for single slip (Mughrabi 1978). It can be seen that the CSSC of the copper multicrystal exhibits a plateau region over a plastic resolved shear range from 6.5×10^{-4} to 4.7×10^{-3} and its cyclic saturation resolved shear stress is about 29–30 MPa, basically equal to that (28–30 MPa) of the copper single crystal (Mughrabi 1978, Cheng and Laird 1981). By the SEM ECC technique, the plastic strain localization in PSBs at a plastic resolved shear strain amplitude of 1.7×10^{-3} was revealed, as shown in figure 2. It is seen that the plastic strain is carried by the PSBs in the copper multicrystal, similar to the observation in single-crystal copper (Winter 1974, Mughrabi 1978). Moreover, it is interesting to note that those PSBs can transfer through the small-angle GBs continuously without the operation of secondary slip. At the higher plastic strain amplitude of 4.7×10^{-3} , dislocation

Table 1. The operating conditions for the SEM ECC technique.

| Acceleration voltage (kV) | Working distance (mm) | Probe (nA) | Brightness (%) | Contrast (%) | Scanning rate |
|------------------------------|--------------------------|---------------|-------------------|-----------------|---------------|
| 20 | 15–22 | 2–5 | 80–98 | 30–33 | TV/2K |

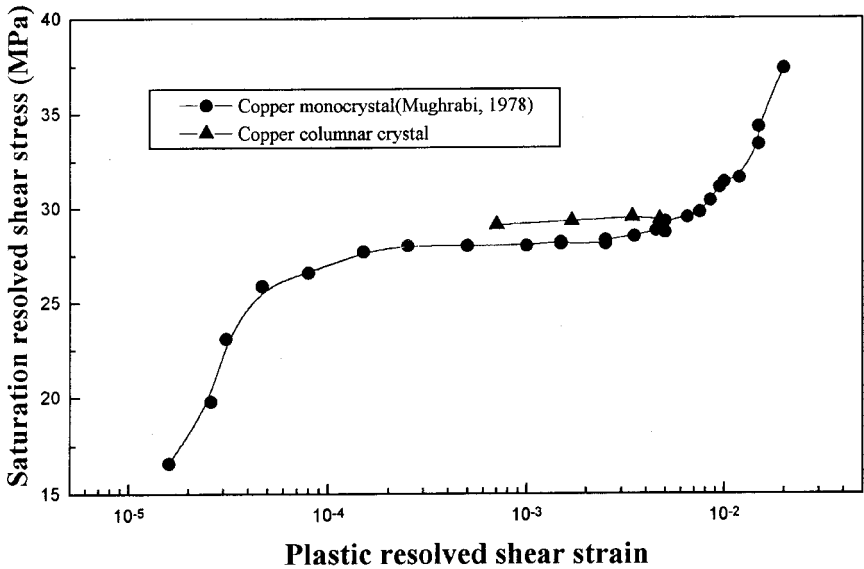


Figure 1. CSSCs of the copper multicrystal and copper single crystal (Mughrabi 1978).

structures evolved into dislocation walls with a width of about $1.5\text{--}1.7\ \mu\text{m}$ throughout the whole specimen, as shown in figure 3. Ladder-like PSBs can be also observed at some sites (see figure 3(a)). Meanwhile, it was found that there was no affected zone in the vicinity of small-angle GBs and the dislocation walls were nearly continuous through the small-angle GBs (see figure 3(b)). These observations are quite different from those for large-angle GBs (Hirth 1972).

3.2. Saturation dislocation patterns in a copper bicrystal

As the bicrystal was cyclically saturated at an axial plastic strain amplitude of 7.6×10^{-4} , its axial saturation stress reached about 63 MPa. The induced saturation dislocation structures within the component grains and near the GB were investigated by the SEM ECC technique. As shown in figure 4(a), the cyclically saturated dislocation pattern in grain G1 $[59\ 13]$ is characterized by a typical two-phase structure consisting of PSB ladders and loop patches. This saturation dislocation pattern is often observed in single-slip oriented copper cyclically deformed in region B of the CSSC (Mughrabi 1978, Laird *et al.* 1986). However, as shown in figure 4(b), the characteristic features of the saturation dislocation pattern within the grain G2 $[579]$ are loop patches or veins which are typical of the structure in region A of the CSSC for single-slip-oriented copper.

Figure 5(a) illustrates the interaction of PSBs with the GB within grain G1. It is interesting to find that PSBs cannot pass through the large-angle GB but produce some affected zones in the neighbouring grain G2 as indicated by arrows. In particular, these affected zones developed along a direction other than the primary slip directions of G1 and G2. They may be preferential sites for initiating fatigue cracks although the physical or mechanical properties of the zones need to be further clarified. Furthermore, as shown in figure 5(b), under higher magnification the ends of the PSBs are seen to become sharper and irregular when they approach

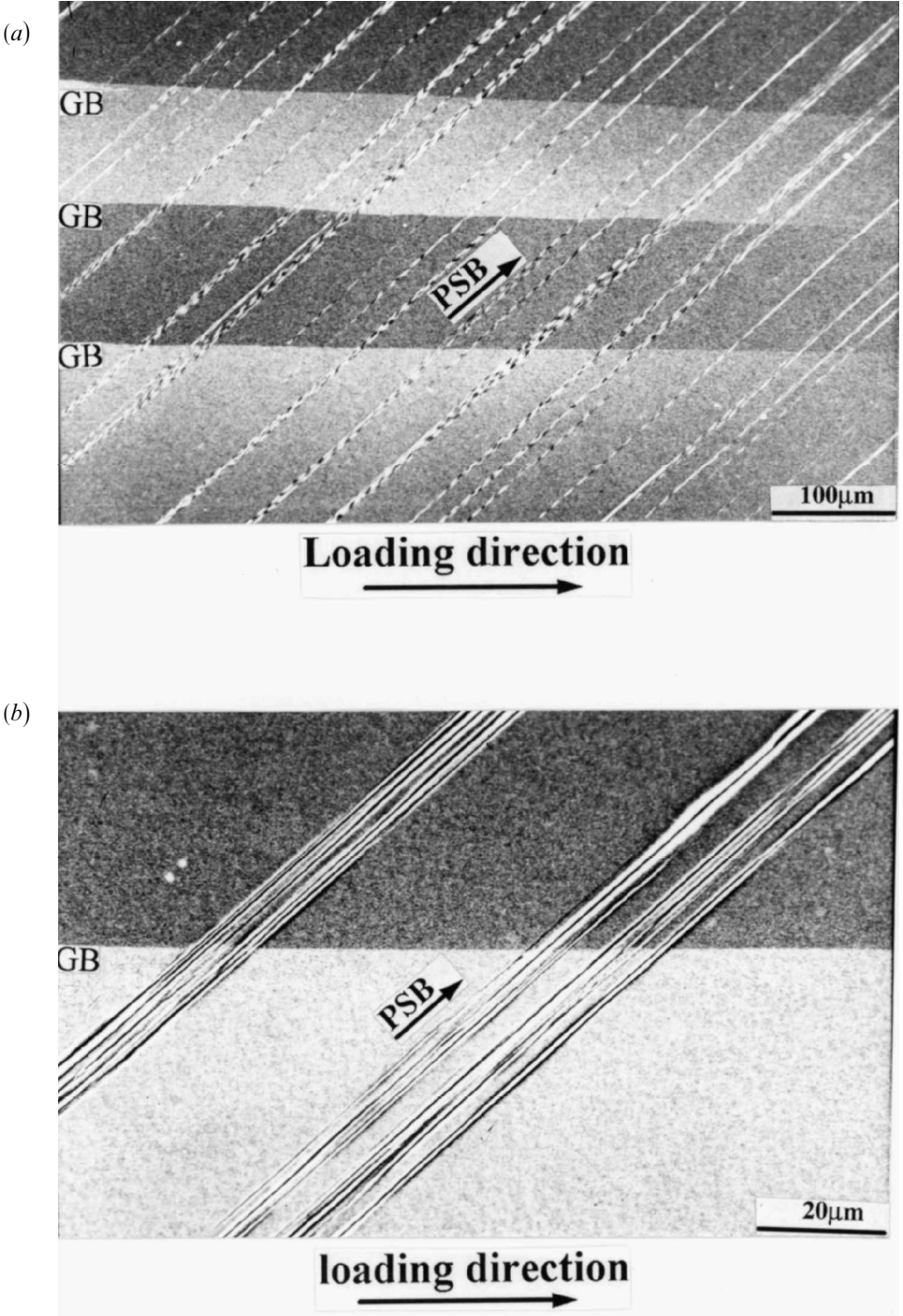


Figure 2. Micrographs (obtained using the SEM ECC techniques showing PSBs passing through the small-angle GBs: (a) low magnification; (b) high magnification. The copper multicrystal specimen was cyclically deformed at axial plastic strain amplitude of 1.7×10^{-3} for 10^4 cycles. It was then polished and recycled at the same strain amplitude for 200 cycles.

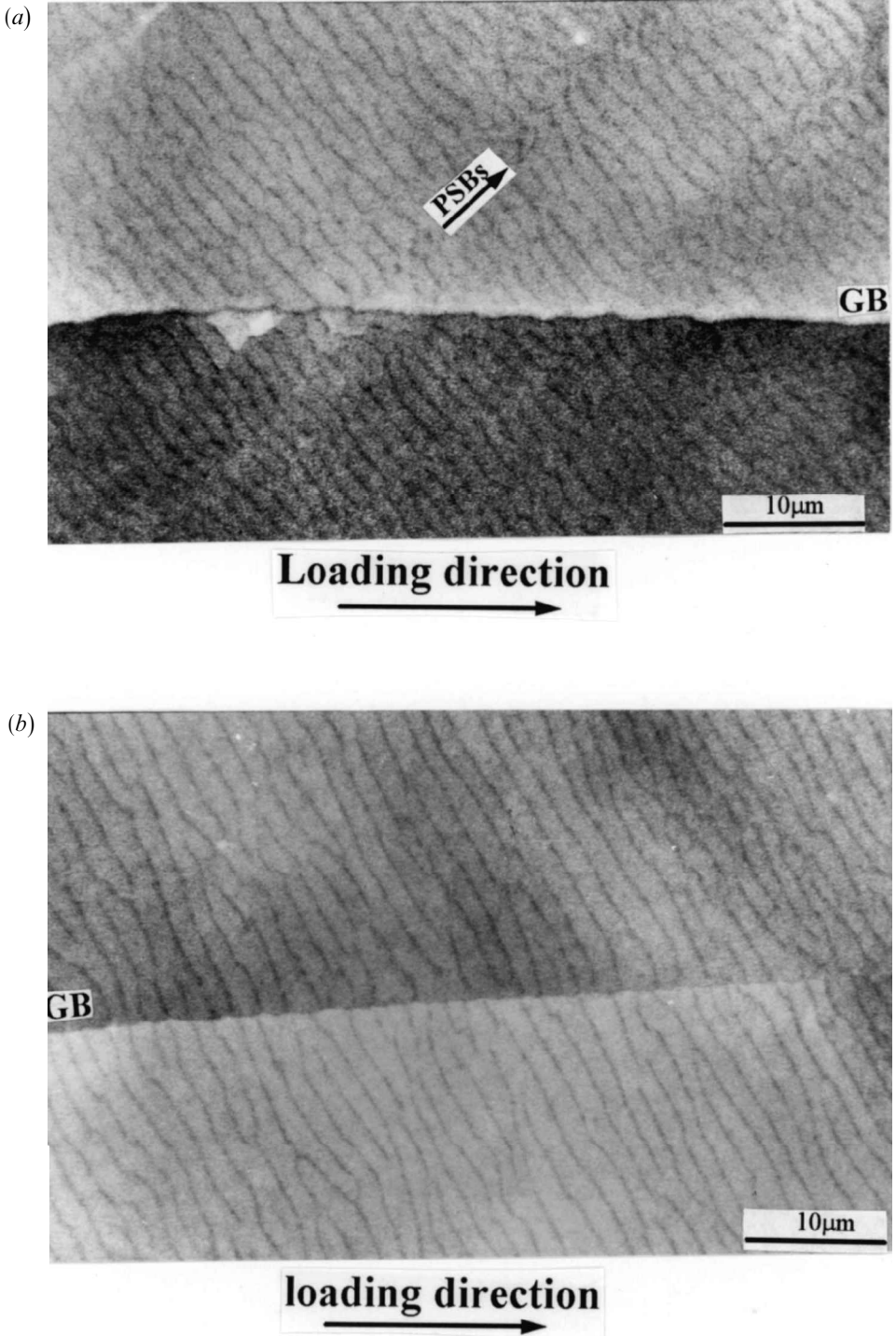
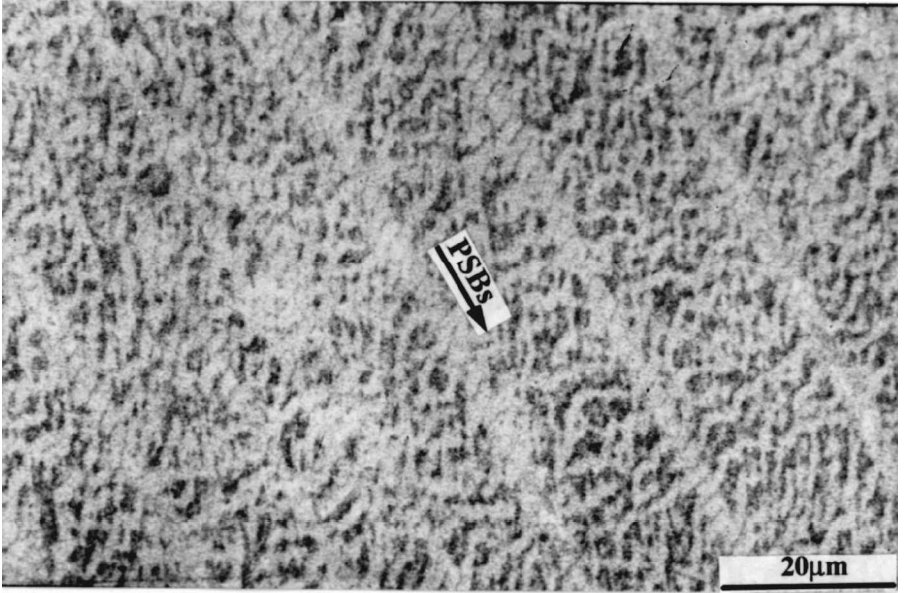


Figure 3. Cyclic saturation dislocation patterns in the vicinity of a small-angle GB in the copper multicrystal cycled at plastic resolved shear strain amplitude of 4.7×10^{-3} for 10^4 cycles, where the loading direction is parallel to the small-angle GB: (a) continuous PSBs and dislocation walls; (b) continuous dislocation walls structures.

(a)



(b)

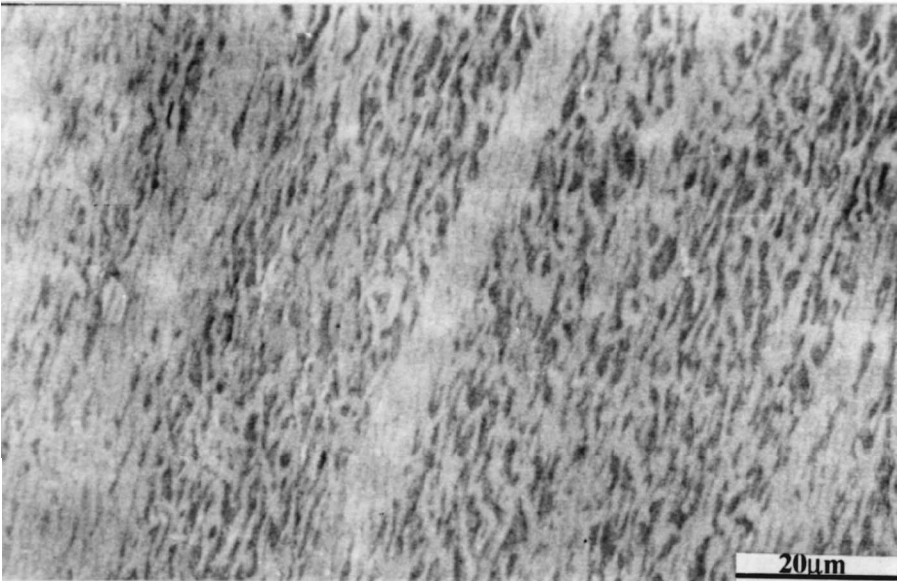


Figure 4. Cyclic saturation dislocation patterns within grains G1 and G2 in the copper bicrystal cycled at an axial plastic strain amplitude of 7.6×10^{-4} for 10^4 cycles: (a) dislocation patterns within component crystal G1 $[5913]$ viewed from plane (814). (b) Dislocation patterns within component crystal G2 $[579]$ viewed from plane (320).

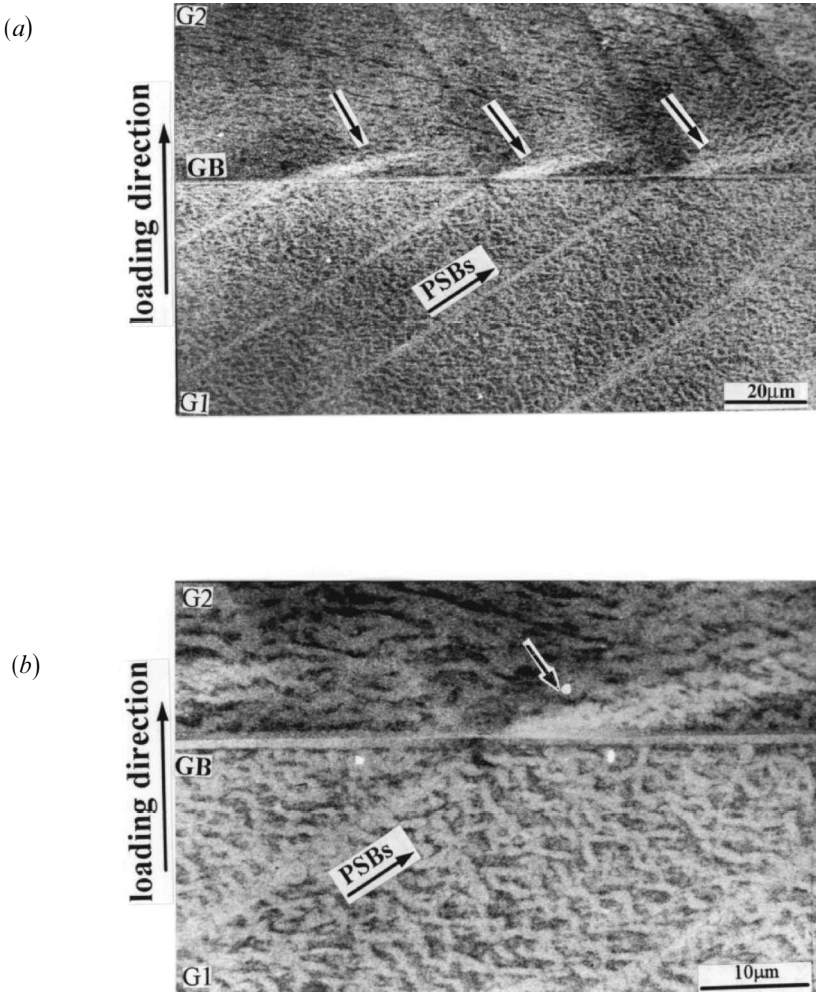


Figure 5. Cyclic saturation dislocation patterns in the vicinity of a large-angle GB in a copper bicrystal cycled at an axial plastic strain amplitude of 7.6×10^{-4} for 10^4 cycles as demonstrated by micrographs (obtained by the SEM ECC technique) showing the interaction of PSBs with large-angle GBs: (a) low magnification; (b) high magnification.

the GB, indicating the existence of stress and strain incompatibility between the component grains G1 and G2 during cyclic deformation.

§ 4. DISCUSSION

4.1. Effect of small-angle grain boundaries on cyclic deformation behaviour

GBs in polycrystals are often considered an important factor in strengthening metals and stress-strain incompatibility at GBs has been discussed extensively (Hirth 1972). However, as the present results indicate, the small-angle GBs seemed to have little effect on the cyclic deformation behaviour in the copper multicrystal. This is easily understood. The cyclic saturation resolved shear stress (29–30 MPa) of the multicrystal is basically equal to that (28–30 MPa) of the copper single crystal

oriented for single slip cyclically deformed in the plateau region. Furthermore, the cyclic saturation dislocation patterns within the grains are similar to those observed in single crystals. The cyclic saturation dislocation patterns can cross through small-angle GBs continuously. It is reasonable to conclude that stress and strain must be compatible at small-angle GBs and no significant strengthening effect exists in copper polycrystal under cyclic loading. The resistance of these small-angle GBs to PSBs may be negligible and the polycrystal behaves quite like a single crystal. This is why the CSSC of the copper polycrystal still exhibited a plateau region even though some small-angle GBs are present (see figure 1).

4.2. Effect of component grain orientations on the formation of persistent slip bands

For the bicrystal with a perpendicular GB, the axial stresses σ_{as} applied to each component grain are equal during cyclic deformation. The resolved shear stresses τ_{as}^{G1} and τ_{as}^{G2} in the primary slip directions of the component grains G1 and G2 respectively will not be the same if the Schmid factors ($\Omega_{G1} = 0.452$; $\Omega_{G2} = 0.406$) of two grains are not equal owing to the difference in their orientations. In fact, the saturation resolved shear stresses τ_{as}^{G1} and τ_{as}^{G2} in the primary slip directions of grains G1 and G2 can be calculated by using the following formulae:

$$\tau_{as}^{G1} = \sigma_{as}\Omega_{G1}, \quad (1)$$

$$\tau_{as}^{G2} = \sigma_{as}\Omega_{G2}. \quad (2)$$

As the bicrystal was cyclically saturated, ε_{pl}^B , ε_{pl}^{G1} and ε_{pl}^{G2} , which are the axial plastic strain amplitudes applied to the bicrystal and to the grains G1 and G2 respectively, will have the following relationship:

$$\varepsilon_{pl}^B = \varepsilon_{pl}^{G1}f_{G1} + \varepsilon_{pl}^{G2}f_{G2}, \quad (3)$$

where f_{G1} and f_{G2} are the volume fractions of the grains G1 and G2 respectively. Taking $f_{G1} = f_{G2} = 0.5$, we have

$$2\varepsilon_{pl}^B = \varepsilon_{pl}^{G1} + \varepsilon_{pl}^{G2}. \quad (4)$$

As reported for a $[\bar{1}49]$ - $[001]$ bicrystal (Peralta and Laird 1997) and according to equations (1) and (2), the component grain G1 with the relatively higher Schmid factor ($\Omega_{G1} = 0.452$) will be subjected to higher resolved shear stress and carry more plastic strain than the component grain G2 with the relatively lower Schmid factor ($\Omega_{G2} = 0.406$), that is

$$\varepsilon_{pl}^{G2} < \varepsilon_{pl}^{G1}. \quad (5)$$

In combination with equations (4) and (5), the following relationship among the plastic strains ε_{pl}^B , ε_{pl}^{G1} and ε_{pl}^{G2} should exist even though the exact values of ε_{pl}^{G1} and ε_{pl}^{G2} are unknown

$$\varepsilon_{pl}^{G2} < \varepsilon_{pl}^B < \varepsilon_{pl}^{G1}. \quad (6)$$

By using equations (1) and (2), the calculated saturation resolved shear stresses τ_{as}^{G1} and τ_{as}^{G2} of the component grains G1 and G2 at an applied axial plastic strain amplitudes of 7.6×10^{-4} are equal to 28.5 MPa and 25.6 MPa respectively. It is known from equation (6) that the axial plastic strain carried by grain G1 will be higher than 7.6×10^{-4} and should be in the range of region B in its CSSC. Therefore,

it is easy to understand why PSBs formed in grain G1 as the bicrystal was cyclically saturated. However, the corresponding dislocation structure within grain G2 is characterized by loop patches or veins (see figure 4(b)) as the bicrystal was cyclically saturated at the axial plastic strain amplitude of 7.6×10^{-4} . The difference in the saturation dislocation patterns of grains G1 and G2 can be explained as follows.

From equation (6), it can be considered that the plastic strain carried by the grain G2 will be below the mean plastic strain amplitude of 7.6×10^{-4} on the bicrystal. In addition, it is generally recognized that the nucleation stress of PSBs in a copper single crystal is in the range 28–30 MPa as the applied plastic strain amplitude was below 10^{-3} (Mughrabi 1978). However, by using equation (2), the calculated saturation resolved shear stress on the primary slip direction of the grain G2 is only equal to 25.6 MPa. This means that the saturation resolved shear stress (25.6 MPa) carried on the grain G2 did not reach the nucleation stress (28–30 MPa) of the PSB within the grain G2. Consequently, as shown in figure 4(b), no typical PSBs formed within the grain G2 even though the ladder-like PSBs have formed within the grain G1 (see figure 4(a)). It is suggested that which component grain is favourable for the PSBs formation depends on its orientation in the bicrystal with a perpendicular GB.

§ 5. SUMMARY AND CONCLUSIONS

The cyclic saturation dislocation patterns within grains and in the vicinity of GBs were observed in a bicrystal and a multicrystal of copper by the SEM ECC technique. The following conclusions can be drawn.

- (1) PSBs and dislocation walls can transfer through the small-angle GBs which showed little effect on the cyclic saturation dislocation patterns and the cyclic saturation stress in the copper multicrystal.
- (2) As the copper bicrystal with a GB perpendicular to the stress axis was cyclically saturated at an axial plastic strain amplitude of 7.6×10^{-4} , PSBs formed only within the component grain G1 with a relatively higher Schmid factor. These PSBs cannot pass through the large-angle GB but produce some affected zones within the adjacent component grain G2.

ACKNOWLEDGEMENT

This work was financially supported by the National Nature Science Foundation of China under grant number 19392300-4. The authors are grateful for this support.

REFERENCES

- BRETSCHNEIDER, J., HOLSTE, C., and TIPPELT, B., 1997, *Acta mater.*, **45**, 3755.
 CHENG, A. S., and LAIRD, C., 1981, *Mater. Sci. Engng*, **51**, 111.
 HIRTH, J. P., 1972, *Metall. Trans. A*, **3**, 3047.
 LAIRD, C., CHARSLEY, P., and MUGHRABI, H., 1986, *Mater. Sci. Engng*, **81**, 433.
 LI, X. W., HU, Y. M., and WANG, Z. G., 1998, *Mater. Sci. Engng* (to be published).
 MELISOVA, O., WEISS, B., and STICKLER, R., 1997, *Scripta mater.*, **36**, 1061.
 MUGHRABI, H., 1978, *Mater. Sci. Engng*, **33**, 207.
 PERALTA, P., and LAIRD, C., 1997, *Acta Mater.*, **45**, 3029.
 SCHWAB, A., BRETSCHNEIDER, J., BUGUE, C., BLOCHWITZ, C., and HOLSTE, C., 1996, *Phil. Mag. Lett.*, **74**, 449.
 SCHWAB, A., MEIBNER, O., and HOLSTE, C., 1998, *Phil. Mag. Lett. A*, **77**, 23.
 WINTER, A. T., 1974, *Phil. Mag. A*, **30**, 719.
 ZAUTER, R., PETRY, F., BAYERLEIN, M., SOMMER, C., CHRIST, H.-J., and MUGHRABI, H., 1992, *Phil. Mag. A*, **66**, 425.